

**Strong motion relation for early-warning application in the Campania region
(Southern Apennines), Italy.**

V. Convertito¹, R. De Matteis³, A. Romeo², A. Zollo² and G. Iannaccone¹

Abstract

For early-warning applications in particular, the reliability and efficiency of rapid scenario generation strongly depend on the availability of reliable strong ground-motion prediction tools. If shake maps are used to represent patterns of potential damage as a consequence of large earthquakes, attenuation relations are used as tool for predicting peak ground-motion parameters and intensities. One of the limitations in the use of attenuation relations is that these have only rarely been retrieved from data collected in the same tectonic environment in which the prediction have to be performed. As a consequence, strong ground motion can result in underestimations or overestimations with respect to the recorded data. This is true also for the Italian territories, and in particular for the Southern Apennines, due to limitations in the available databases, both in terms of distances and magnitude. Moreover, for “real-time” early-warning applications, it is important to have attenuation models for which the parameters can be easily upgraded when new data are collected, whether this has to be done during the earthquake rupture occurrence or in the post-event, when the whole strong motion waveforms are available.

In the present study, a strong-motion attenuation relation for early-warning applications in the Campania region (Southern Apennines), Italy, is presented. The model has a classical analytical formulation, and its coefficients were retrieved from a synthetic strong-motion database created by using a stochastic approach. The input parameters for the simulation technique were obtained through the spectral analysis of waveforms of earthquakes recorded by the Istituto Nazionale di Geofisica e Vulcanologia (INGV) network for a magnitude range M_d (1.5,5.0) in the last fifteen years, and they have been extrapolated to cover a larger range.

To validate the inferred relation obtained, comparisons with two existing attenuation relations are presented. The results show that the calibration of the attenuation parameters, i.e., geometric spreading, quality factor Q , static stress drop values along with their uncertainties are the main concern.

Introduction

The prediction of strong ground-motion parameters in both the time and frequency domains is of fundamental importance for seismic hazard analyses and for seismic early-warning applications. The reliability of the predictions depends mainly on the ability to model all of the aspects that can affect the radiated energy at the source during its propagation to the sites of interest.

Although many prediction methods exist (e.g., empirical Green's functions, semi-empirical, semi-theoretical, stochastic and theoretical), the widest used in almost all earthquake-prone regions are those based on an empirical approach. Empirical models, which are generally referred to as attenuation relations, are mathematical functions that relate the selected strong ground-motion parameter (peak ground acceleration, velocity and displacement or spectral ordinates) to parameters characterizing the source, the medium (in terms of geometric spreading and anelastic absorption and scattering) and the local site geology (Campbell, 1985). Once the functional form has been selected, the coefficients are retrieved using regression analysis on an existing strong-motion database.

When attenuation relations are used for predicting ground motion, one of the major prerequisites is that the estimates should be used only for regions in which the data are collected or for regions that based on geophysical and seismological data, have similar source and propagation characteristics (Reiter, 1990). However, the absence of large and complete databases, in terms of magnitude, distances and fault mechanisms, represents a serious problem in such cases. Moreover, the intrinsic limitations of a point-like description of the seismic source must be considered, in particular when ground motion due to a large earthquake in the near-source range has to be estimated. In fact, these motions are strongly affected by source duration and geometry, which cannot be taken into account in attenuation relations.

The Campania region is located in the Southern Apennines of Italy, and there have been several large destructive earthquakes in recent times. The last of these was the 1980 M 6.9 Irpinia earthquake, which caused several thousand deaths and resulted in severe economic losses. This

region is now covered by an advanced network that is equipped with highly dynamic and densely spaced instruments that will allow the registration of non-saturated time histories from a broad-band spectrum of magnitude (Weber *et al.*, 2006, this issue). The network is mainly devoted to early-warning seismic purposes, and due to its geometric characteristics it is designed to provide rapid damage scenarios through the calculation of shake maps. These maps are simple or sophisticated representations of the ground shaking in terms of a selected strong ground-motion parameter that results from large earthquakes. As a consequence, the formulation of a regional attenuation relation is of great concern.

The present study is aimed at retrieving a strong motion relation for the Campania region as a possible alternative to those already existing that were developed for the Italian territory recently (Sabetta and Pugliese, 1987; Sabetta and Pugliese 1996; Malagnini *et al.*, 2000). The results presented here refer to the peak ground acceleration (Pga) and peak ground velocity (Pgv), but they can be extended to other time or spectral parameters. The major difficulty was the absence of a strong ground-motion database recorded in the area of interest. Thus, to partially overcome this difficulty, we analyzed a database of waveforms recorded from 1988-2003 by the INGV network for a magnitude range M_d (1.5,5.0). Although these data do not provide the required strong-motion database, they do allow the retrieval of local scaling laws (i.e., seismic moment vs corner frequency; static stress drop vs corner frequency) and anelastic characteristics that can be extrapolated for larger earthquakes and the production of a synthetic database using a stochastic simulation procedure. This database can thus be used both to complete existing limited databases and to directly retrieve local attenuation relations.

Database and scaling laws

One of the major problems to be faced when a local attenuation relation is to be retrieved is the absence of a large and complete strong-motion database. This can be partially overcome using a

simulation technique that is able to generate waveforms with the spectral and temporal characteristics of interest. The technique adopted in the present study is the stochastic simulation method that was proposed by Boore (1983), which requires as input parameters the static stress drop and corner frequency for a selected range of earthquake magnitudes. To infer these parameters for the Campania region, local scaling laws were obtained by analysing the earthquake waveforms recorded by the INGV network from 1988 to 2003 with magnitude between 1.5 and 5.0 (Figure 1). We selected only the earthquakes recorded at least at six seismic stations with a clear P-wave phase. Then, starting from an original catalogue of 788 earthquakes, we extracted for the following analyses 2,774 waveforms of earthquakes in the magnitude range M_d (1.8,4.5). We performed the picking of the first P- and S-wave arrival times and re-located the events in a flat-layered velocity model proposed by Bernard and Zollo (1989).

The classic ω^{-2} Brune (1970) spectral model is used to estimate the source parameters Ω_0 (low-frequency spectral amplitude), f_c (corner frequency) and Q_P (quality factor) by the inversion of displacement spectra. Since the seismic stations of the INGV network are, for the most part, equipped with single vertical component sensors, only the P-wave spectra were inverted.

The displacement spectrum was calculated on a 1-s window, around the first P-wave arrival time (panels a and b of Figure 2). The window width was chosen taking into account the distance and magnitude ranges covered in the database. The non-linear inversion technique used is based on the Simplex optimization method (Nelder and Mead, 1965), which requires a reference starting model. It is a local search method based on the minimization of a cost function defined as the absolute value of the observed minus the predicted spectrum, multiplied by the square of the frequency. To overcome the problem to fall in local minima, several inversions were performed with different initial model parameters that were chosen randomly in reasonable ranges. This avoided an arbitrary selection criterion for the starting model. As an example, the initial and final values for Ω_0 , f_c and Q_P obtained after the P-wave spectral inversion are shown in Figure 3.

The retrieved parameters were finally used to estimate the relations between seismic moment, stress drop and corner frequency (Figure 4), which can be used as input parameters for the stochastic simulation technique when large earthquakes need to be simulated.

For the quality factor Q_p , the results of the inversion procedure show a linear source-to-station distance dependence (Figure 5). This could be ascribed to incorrect modeling of the geometric attenuation effect in our spectral model. To minimize this effect in the simulation of the strong ground motion, the dependence was introduced into the stochastic approach, as detailed further in the next section.

Peak ground-motion simulation

To set up a database for the distance and magnitude ranges of interest regarding the seismotectonics of the Campania region, the stochastic simulation technique introduced by Boore (1983) was used to generate synthetic time histories of motion, from which the Pga and Pgv values were calculated. This technique works in both the time and frequency domains, and it is based on the generation of a time sequence of filtered and windowed, band-limited, Gaussian noise with zero expected mean and variance chosen to give unity as spectral amplitude. This spectrum is then multiplied by a specified spectrum (e.g., Brune, 1970) and the transformation back to the time domain yields the final time series.

The technique proposed by Boore (1983) allows for the selection of several acceleration spectrum shapes, taking into account the source, attenuation (geometric, anelastic and superficial) and site effects. In the present application, the following formula for the acceleration spectrum $A(f)$ was used:

$$A(f) = CM_0 S(f, fc) \frac{e^{\frac{\pi R}{Q\beta}}}{R} \quad (1)$$

where R is the epicentral distance and C is a constant given by:

$$C = \frac{R_{\theta\phi} \cdot FS \cdot P}{4\pi\rho\beta^3} \quad (2)$$

$R_{\theta\phi}$ is the mean radiation pattern, which is assumed to be 0.63 for shear waves; FS is the amplification due to the free surface (taken as 2.0 here); P is the reduction factor that accounts for the partitioning of the energy into two horizontal components (taken as $1/\sqrt{2}$ here); and ρ and β are the density and shear-wave velocity.

The shape of the source spectrum is the classical ω^{-2} Brune (1970) model with a single corner frequency f_c :

$$S(f, f_c) = \frac{f^2}{1 + \left(\frac{f}{f_c}\right)^2} \quad (3)$$

For the geometric spreading, due to the aim of the present study, it was assumed to have a functional form that accounts for the S -wave geometric spreading up to 300 km, and then for the surface-wave geometric spreading. This is specified through a distance function $g(r)$ that follows the following expression:

$$g(r) = \begin{cases} r^{-1.0} & 1 \leq r \leq 300 \text{ km} \\ r^{-0.5} & r > 300 \text{ km} \end{cases} \quad (4)$$

The effect of anelastic attenuation was considered by allowing for a frequency dependence of the type:

$$Q(f) = Q_0 \left(\frac{f}{f_0} \right)^n \quad (5)$$

where f_0 is a reference frequency, and n is a parameter controlling the difference in the attenuation of low and high frequency components. Following previous studies for the same region (i.e., Rovelli *et al.*, 1988; Malagnini *et al.*, 2000), f_0 was assumed to be 1.0 Hz and n was fixed at 1.0 (both of these previous studies assumed f_0 to be 1.0 Hz, while Malagnini *et al.* (2000) assumed n to be 0.1).

The selection of the Q_0 reference value in equation (5) was based on the analysis of the results obtained from the P-wave spectra inversion, and it is shown in Figure 5. From Figure 5, a distance dependence of the Q factor can be seen, which must be taken into account in equation (5). As mentioned in the previous section, this result can be ascribed to an intrinsic trade-off between the implicitly assumed $1/r$ geometric spreading and a frequency independence of the Q factor in the spectrum inversion. As a consequence, equation (5) was reformulated to the following expression:

$$Q(r, f) = (Q_0 + Kr) \left(\frac{f}{f_0} \right)^n \quad (6)$$

This can simply be introduced into the Boore (1983) simulation technique. In particular, Q_0 and K were estimated using linear regression analysis, and were 77 ± 13 and $2.10 \pm 0.01 \text{ km}^{-1}$, respectively. No kappa filter (Anderson and Hough, 1984) was used to account for attenuation of ground motion due to surface layers because of the aim of the present study: to obtain ground motion estimates relative to rock-site conditions.

The last parameters to be specified for the simulation are the seismic moment M_0 and static stress drop $\Delta\sigma$, which can be considered either magnitude dependent or independent. Based on the results shown in Figure 4a, a magnitude independence can be assumed for $\Delta\sigma$. On the other hand, for each fixed magnitude, three values of stress drop were used. The median value and the values corresponding to ± 1 standard deviation (see Figure 4a) were selected to take into account uncertainties in the estimated stress drop values and to introduce a further variability into the peak ground-motion values.

The synthetic database for Pga and Pgv for M 5, 6 and 7 and for distances ranging between 5 and 150 km is shown in Figure 6a, b, respectively. The values were calculated with reference to rock-site conditions. To partially verify the correctness of the parameters selected for the stochastic simulation procedure, the same Figure includes the Pga and Pgv values (black crosses) corresponding to two aftershocks of the 23 November 1980/18:34 M 6.9 Irpinia earthquake: the 01 December 1980/19:04 M 4.6 and 16 January 1981/00:37 M 4.7 earthquakes. As seen from Figure 6, the simulated peak values are in good agreement with the observed data for both Pga and Pgv.

The generated database allowed to formulate the attenuation model and to compute the coefficients for predicting strong ground motion.

Regression analysis

Once the simulation had been calibrated for the region of interest, in terms of attenuation (geometric and anelastic) and static stress drop conditions, a synthetic database for a fixed range of magnitude and distances of interest was generated. This synthetic data can be used both to integrate existing databases and to retrieve *ad-hoc* regional attenuation relations for strong motion parameters.

This approach was preferred to those based on attenuation models for the Fourier spectrum (Toro *et al.*, 1997; Rovelli *et al.*, 1988; Malagnini *et al.*, 2000) due to the aim of the present study. In fact, for early-warning applications, scenarios that represent parameters that can be correlated to

structural damage need to be provided rapidly to the civil protection authorities. Although the response spectrum provides the most interesting engineering parameters, Pga and Pgv still remain the most used ones.

In the present study, a synthetic database was used to retrieve an *ad-hoc* attenuation relation that can be easily upgraded when new data are available, whether during the earthquake occurrence or in a post-event stage, for the formulation of shake maps.

A classical attenuation model for the peak ground parameter was assumed (e.g., Joyner and Boore, 1981; Campbell, 1997; Sabetta and Pugliese, 1996; Abrahamson and Silva, 1997; Boore *et al.*, 1997), the formulation for which is as follows:

$$\log_{10} Pgx = a + bM + c \log_{10} \sqrt{R^2 + h^2} \pm \sigma \quad (7)$$

where Pgx corresponds to both Pga and Pgv; M is magnitude; R is the epicentral distance in kilometres; h is a fictitious depth value in kilometres; and σ is the standard deviation of the logarithm of Pgx. The selected model assumes an exponential function of the magnitude that comes from the basic definition of magnitude as the logarithmic measure of the ground-motion amplitude (Campbell, 1985), and a geometric spreading $1/R$, and h accounts for the property normally referred to as “saturation with distance” (Joyner and Boore, 1981; Campbell, 1985). The model assumed does not account for site effect, in so far as this effect is introduced *a-posteriori* in the shake maps using particular soil classifications (e.g., QTM) and coefficients of amplification for the selected strong ground-motion parameter (Wald *et al.*, 1999).

To fit the database for each magnitude, the c parameter was fixed during the inversion, while the a and b parameters were allowed to vary. Using a trial-and-error procedure, c was found to be -1.4 and h was found to be 5.5 km for Pga and 5.0 km for Pgv. The difference in the h values accounts for the different attenuation when the different ranges of frequencies to which Pga and Pgv belong are considered.

The best estimates for the a and b parameters, with the relative uncertainties obtained using the ordinary least-squares analysis, are given in Table 1, along with the standard deviation of the logarithm of P_{gx} .

Figures 7 and 8 show the attenuation relations for M 5, 6 and 7 (continuous lines) and the databases for P_{ga} and P_{gv} (grey squares), respectively. For comparison, the other two attenuation laws for the same magnitude are given on the same Figures. The dashed lines represent the attenuation curves of Sabetta and Pugliese (1996) (hereinafter: SP96), while the dotted lines represent the attenuation curves of Campbell (1997) (hereinafter: CA97). The selection of these two attenuation relations was based on the fact that the SP96 attenuation relation was retrieved from an Italian strong motion database that contained normal and thrust fault mechanisms prevalently, while the CA97 attenuation relation was retrieved from a worldwide database that included different seismotectonic environments and a larger number of faulting styles. The comparisons between the different curves show that the attenuation relation retrieved in the present study and in CA97 have similar behaviours for distances greater than 20 km in terms of attenuation, but they provide different ground-motion estimates. Thus, CA97 provides larger estimates for P_{ga} and P_{gv} for each magnitude, except for P_{gv} and M 7. On the other hand, the comparison with SP96 shows different behaviours in terms of both the peak ground-motion estimates and the trend of the attenuation. This further stresses the need to retrieve attenuation relations from data collected in the same region in which the estimates are performed.

Panels b and c of Figures 7 and 8 show the residuals (observed minus predicted P_{ga} values) versus magnitude for each of the attenuation relations, where the circles in panels b represent the residuals relative to the attenuation relation calculated in the present study, with panels c showing the residuals relative to the SP96 (crosses) and CA97 (diamonds) attenuation relations. The results show that the attenuation relation inferred in the present study provides estimates that are consistent with those of SP96, but smaller than those of CA97, in particular, for larger magnitude.

To validate the assumed regression model of equation (7) and the computed coefficients given in Table 1, a further test was performed using the data relative to the 23 November 1980/18:34 M 6.9 Irpinia earthquake, where the residuals analysis was re-performed in a two-stage approach. In the first stage, the estimates obtained using the retrieved regression model in the present study for magnitude M 6.9 and epicentral distances for which data are available were compared. The results are shown in Figures 9 and 10 for Pga and Pgv, respectively. In panels a of both of these Figures, the triangles represent the available data and the circles represent the estimates, for the same distances, obtained with the attenuation relation retrieved in the present study. On the same panels, the estimates obtained using the attenuation relations of SP97 (crosses) and CA97 (diamonds) are also shown, while the lines refer to a continuous range of distances and a magnitude M 6.9. The style used for these lines corresponds to that shown in Figure 7. The corresponding residuals are shown in Figures 9b and 10b.

In the second stage of the analysis, the data of the 23 November 1980/18:34 M 6.9 Irpinia earthquake were added to the synthetic database and the regression analysis re-performed, to have the same starting information for the three different attenuation relations. The new retrieved coefficients and relative uncertainties are given in Table 2, both for Pga and Pgv. It can be seen that there are only slight variations in the coefficients, while the uncertainties remain the same. The corresponding attenuation curves for Pga and Pgv are shown in Figures 9 and 10, respectively (dashed bold lines). The estimates for each single data point and the residuals are also given (black inverted triangles on panels b of the same Figures). As expected, from the analysis of the residuals, the introduction of the data relative to the 23 November 1980/18:34 M 6.9 Irpinia earthquake into the synthetic database partially improved the estimates.

Conclusions

In the present study, an *ad-hoc* attenuation relation for the Campania region of the Southern Apennines (Italy) has been retrieved. The regression model is reported in equation (7) and the coefficients to use for the prediction are reported in Table 2. The aim of the present study was driven by on-going realisation of a dense seismic array in the Campania Region for early warning and rapid shake map evaluation purposes.

Due to the absence of a large and complete strong motion database, a spectral analysis was performed on earthquake waveforms recorded from 1988-2003 by the INGV network for a magnitude range M_d (1.5,5.0). This allowed to obtain scaling laws, i.e., seismic moment vs corner frequency, and static stress drop vs corner frequency, which can be extrapolated for larger magnitude values. The inferred parameters were then used as the input for the stochastic simulation technique proposed by Boore (1983), to calculate the synthetic waveforms and the associated Pga and Pgv values for the magnitude range of interest (M 5,6 and 7).

Once the database had been built, regression analysis and comparison tests of the residuals were performed. The estimates obtained by the attenuation relation retrieved in the present study were compared with those obtained by two other existing relations. The results show that Pga and Pgv are substantially in agreement, while there are different trends in the attenuation (geometric and analeptic), thus stressing the need to retrieve attenuation relations with data that has been collected in the same region in which the estimates are to be performed.

Acknowledgments

The Figures were prepared with Generic Mapping Tools (Wessel and Smith, 1991).

References

- Abrahamson, N. A., and W. J. Silva (1997). Empirical response spectral attenuation relations for shallow crustal earthquakes, *Seism. Res. Lett.* **68**, 94-127.
- Anderson, J. G., and S. E. Hough (1984). A model for the shape of the Fourier amplitude spectrum acceleration at high frequencies, *Bull. Seism. Soc. Am.* **74**, 1969-1993.
- Bernard P. and A. Zollo (1989). The Irpinia (Italy) 1980 earthquake: detailed analysis of a complex normal faulting. *J. Geophys. Res.*, **94**, 1631-1648.
- Boore, D. M. (1983). Stochastic simulation of high-frequency ground motion based on seismological models of the radiated spectra, *Bull. Seism. Soc. Am.* **73**, 1865-1893.
- Boore, D. M., W. B. Joyner, and T. E. Fumal (1997). Equations for estimating horizontal response spectra and peak acceleration from Western North American earthquakes: a summary of recent work, *Seism. Res. Lett.*, **68**, 128-153.
- Brune, J. (1970). Tectonic stress and spectra of seismic shear waves from earthquakes, *J. Geophys. Res.*, **75**, 4,997-5,009.
- Campbell, K.W. and M. EERI (1985). Strong Motion Attenuation Relations: A Ten-Years Perspective. *Earthquake Spectra*, Vol. 1, No. 4.
- Campbell, K.W. (1997). Empirical Near-Source Attenuation Relationships for Horizontal and Vertical Components of Peak Ground Acceleration, Peak Ground Velocity, and Pseudo-Absolute Acceleration Spectra. *Seism. Res. Lett.*, **68**, 154-179.
- Joyner, W. B., and D. M. Boore (1981). Peak horizontal acceleration and velocity from strong-motion records including records from the 1979 Imperial Valley, California earthquake, *Bull. Seism. Soc. Am.* **71**, 2011-2038.
- Malagnigni, L., Herrmann R. B. and M. Di Bona (2000). Ground-Motion Sacling in the Apennines (Italy), *Bull. Seism. Soc. Am.* **90**, 1062-1081.
- Nelder, J.A., and Mead, R. (1965). A simplex method for function minimization. *Computer Journal*, vol. **7**, p. 308.

- Reiter, L. (1990). *Earthquake hazard analysis-Issues and Insights*, Columbia University Press, New York, 254 pp.
- Rovelli, A., O. Bonamassa, M. Cocco, M. Di Bona, and S. Mazza (1988). Scaling laws and spectral parameters of the round motion in active extensional areas in Italy, *Bull. Seism. Soc. Am.* **78**, 530-560.
- Sabetta, F. and A. Pugliese (1987). Attenuation of peak horizontal acceleration and velocity from Italian strong-motion records, *Bull. Seism. Soc. Am.* **77**, 1491-1513.
- Sabetta, F., and A. Pugliese (1996). Estimation of Response Spectra and Simulation of Nonstationary Earthquake Ground Motions, *Bull. Seism. Soc. Am.* **86**, 337-352.
- Toro R., N.A. Abrahamson, and J. F. Schneider (1997). Model of Strong Ground Motions from Earthquakes in Central and Eastern North America: Best Estimates and Uncertainties. *Seism. Res. Lett.*, **68**, 41-57.
- Wald D. J., Quitoriano V., Heaton T. H., Kanamori H., Scrivner C.W., and Worden B.C. (1999). TriNet "ShakeMaps": Rapid Generation of Peak Ground Motion and Intensity Maps for Earthquake in Southern California, *Earthquake Spectra*, **15**, 537-555.
- Weber E., Iannaccone G., Zollo A., Bobbio A., Cantore L., Corciulo M., Convertito V., Di Crosta M., Elia L., Emolo A., Martino C., Romeo A. and Satriano C. (2006). Development and testing of an advanced monitoring infrastructure (ISNet) for seismic early-warning applications in the Campania region of southern Italy. This issue.
- Wessel, P., and W. H. F. Smith (1991). Free software helps map and display data, *EOS Trans. AGU* **72**, 441, 445-446.

Affiliation

1. Istituto Nazionale di Geofisica e Vulcanologia

Osservatorio Vesuviano

Napoli, Italy

2. Dipartimento di Scienze Fisiche

Università degli Studi “Federico II” di Napoli

Napoli, Italy

3. Dipartimento di Studi Geologici ed Ambientali

Università degli studi del Sannio

Benevento, Italy

Tables

Table 1: Regression coefficients and standard errors of equation (7) for Pga and Pgv

Pgx	a	b	c	h	σ
$Pga \text{ (m/s}^2\text{)}$	-0.514 ± 0.007	0.347 ± 0.001	-1.4	5.5	0.145
$Pgv \text{ (m/s)}$	-3.04 ± 0.01	0.552 ± 0.002	-1.4	5.0	0.154

Table 2: Regression coefficients and standard errors of equation (7) for Pga and Pgv following the addition to the synthetic database of the data from the 23 November 1980/18:34 M 6.9 Irpinia earthquake.

Pgx	a	b	c	h	σ
$Pga \text{ (m/s}^2\text{)}$	-0.559 ± 0.007	0.383 ± 0.001	-1.4	5.5	0.155
$Pgv \text{ (m/s)}$	-3.13 ± 0.01	0.570 ± 0.002	-1.4	5.0	0.185

Figure Legends

Figure 1: Map of the INGV seismic stations (black triangles) and the epicentral distribution of the earthquakes analysed (black dots).

Figure 2: (a) Vertical component of velocity; (b) Selected time window; (c) Observed (black line) and inverted (red line) amplitude displacement spectra.

Figure 3: (a) (d) (g) Starting values for the Ω_0 , f_c and Q_P parameters, respectively, used in the inversion procedures; (c) (f) (i) Final values for Ω_0 , f_c and Q_P , respectively, after the inversion; (b) (e) (h) Histograms of the final values for Ω_0 , f_c and Q_P , respectively (red bars) and their corresponding modal values (black triangles).

Figure 4: Retrieved scaling laws: (a) Static stress ($\Delta\sigma$) drop vs corner frequency. The continuous line represents the median and the dotted lines represent ± 1 standard deviations. (b) Seismic moment vs corner frequency. The continuous line represents the median and the dotted lines represent ± 1 standard deviations.

Figure 5: The Q_P values retrieved from the spectral P-waveform inversion as a function of the epicentral distance. Continuous and dotted lines as for Figure 4.

Figure 6: (a, b) Synthetic databases for P_{ga} and P_{gv} , respectively, as functions of the epicentral distances for M 5, 6 and 7. The crosses refer to the data of the November 1980/18:34 M 6.9 Irpinia earthquake and the 01 December 1980/19:04 M 4.6 and 16 January 1981/00:37; M 4.7 aftershocks.

Figure 7: (a) Attenuation curves for Pga for M 5, 6 and 7: The continuous lines correspond to the attenuation relation retrieved in the present study, the dashed to that of SP96, and the bold dashed to CA97. (b) Residual analysis for the attenuation relation retrieved in the present study. (c) Residual analysis for the SP96 (crosses) and CA97 (rhombuses) attenuation relations.

Figure 8: As for Figure 7, but for Pgv.

Figure 9: Validation test for Pga: (a) The triangles represent the observed data of the November 1980/18:34 M 6.9 Irpinia earthquake, the circles represent the estimates of the attenuation relation retrieved in the present study, the crosses correspond to the estimates of the SP96 attenuation relation, and the rhombuses correspond to the estimates of the CA97 attenuation relation. The inverted black triangles correspond to the estimates of the attenuation relation retrieved in the present study when the observed data of the November 1980/18:34 M 6.9 Irpinia earthquake were added to the synthetic database. The lines show the continuous ranges of distances; see legend to Figure 7 for details. (b) Residual analysis for the validation test. Symbols as for panel (a).

Figure 10: As for Figure 9, but for Pgv.

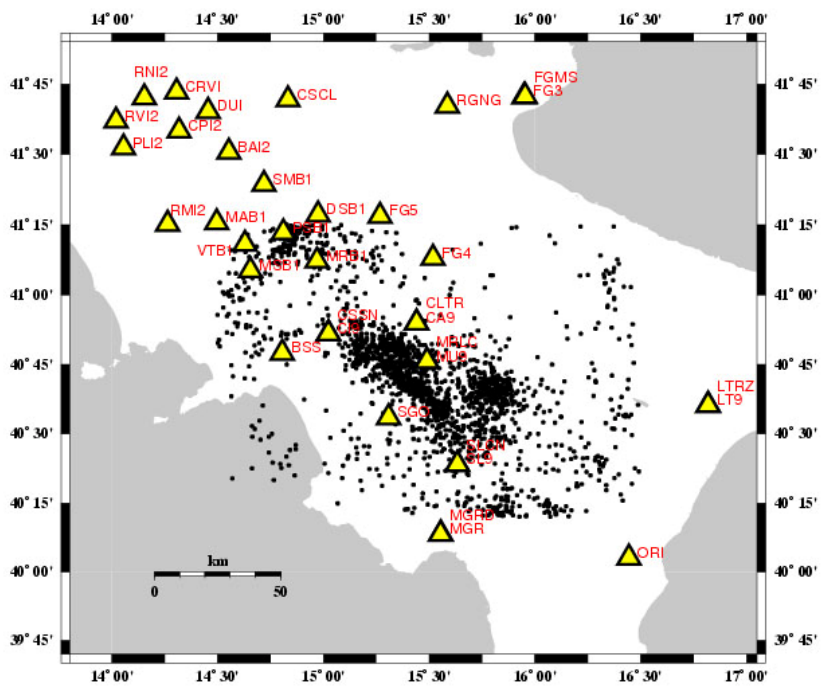


Fig.1

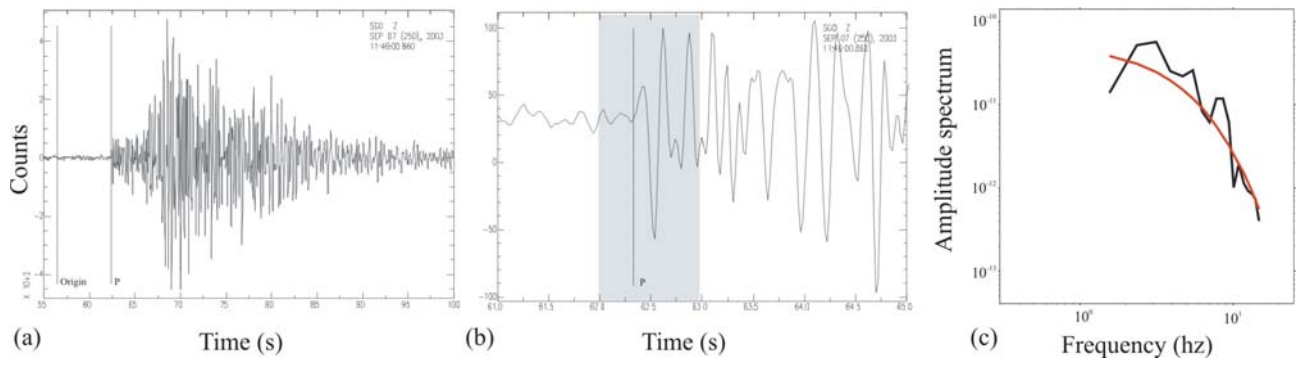


Fig.2

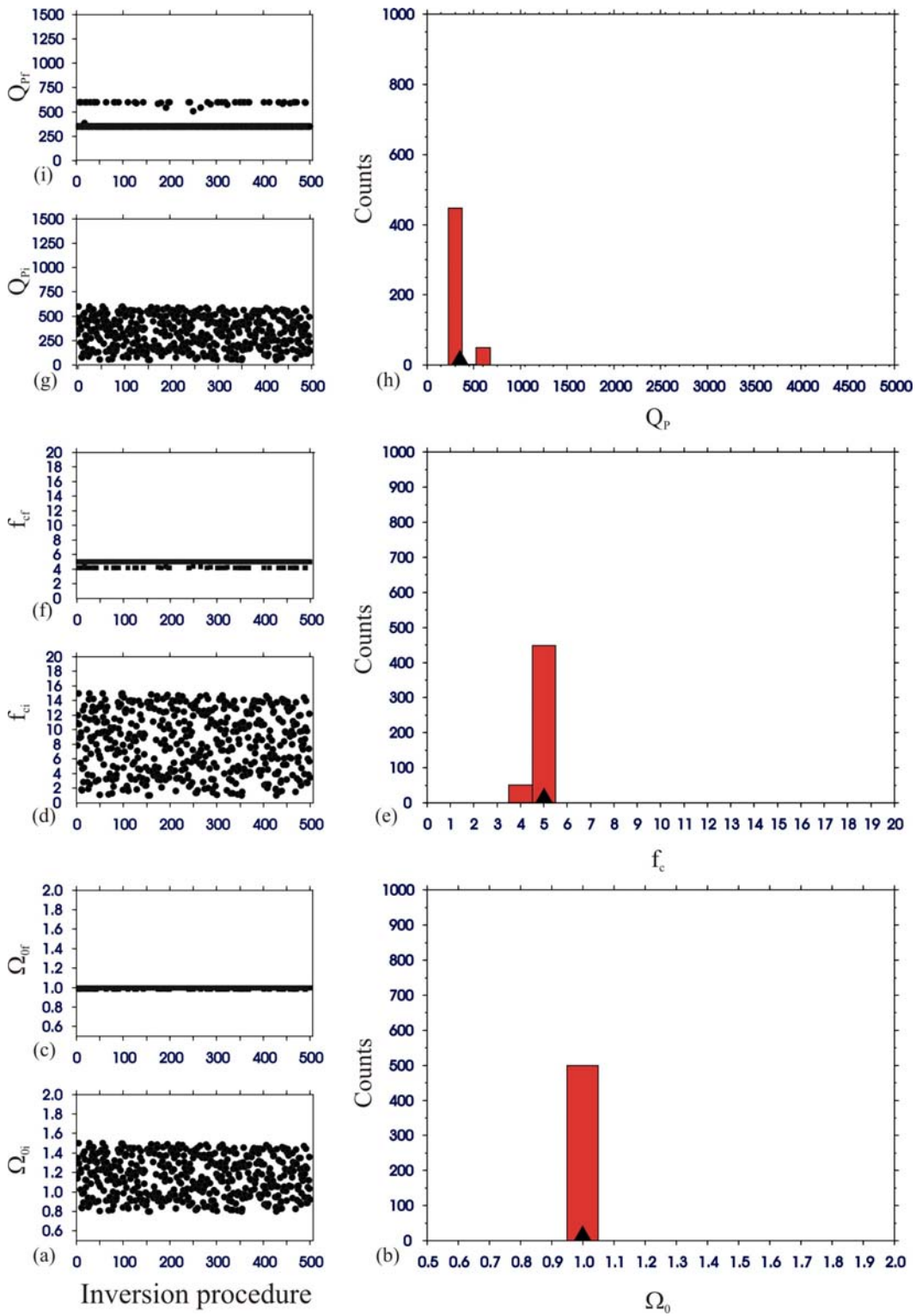


Fig.3

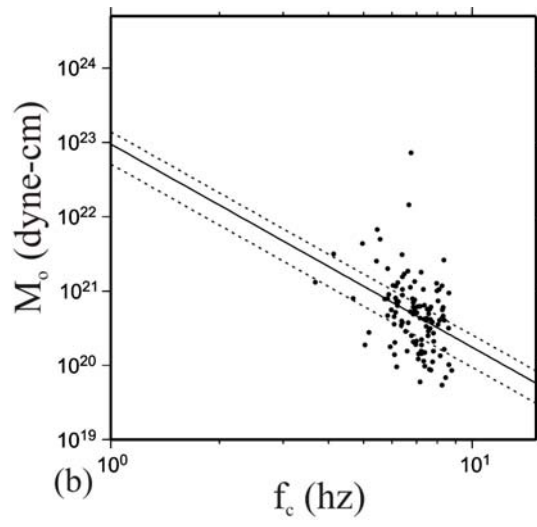
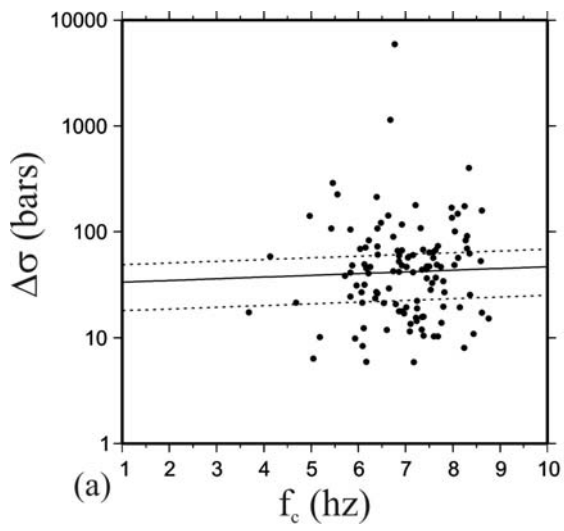


Fig.4

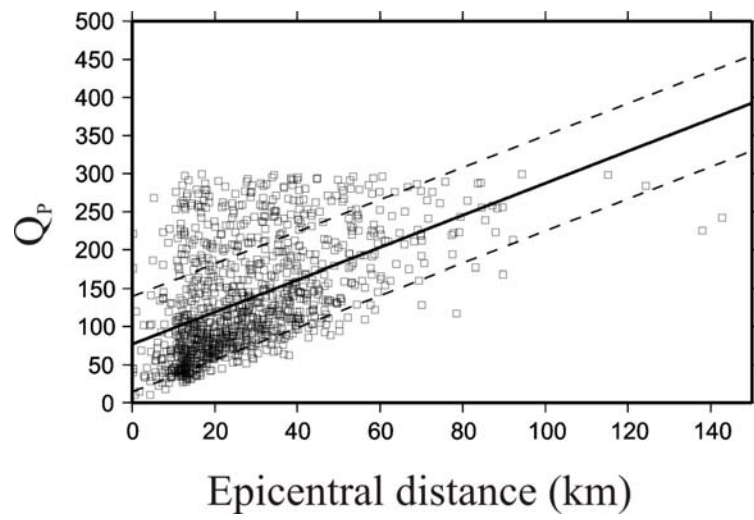


Fig. 5

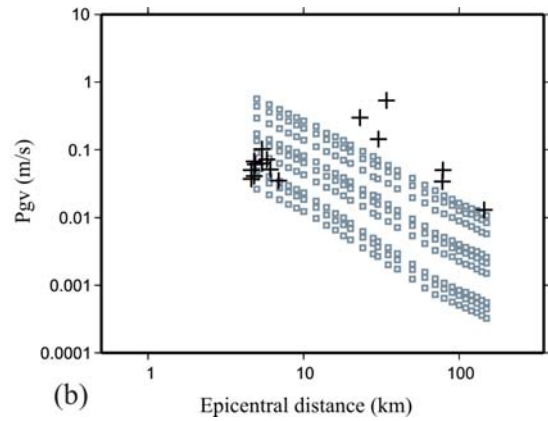
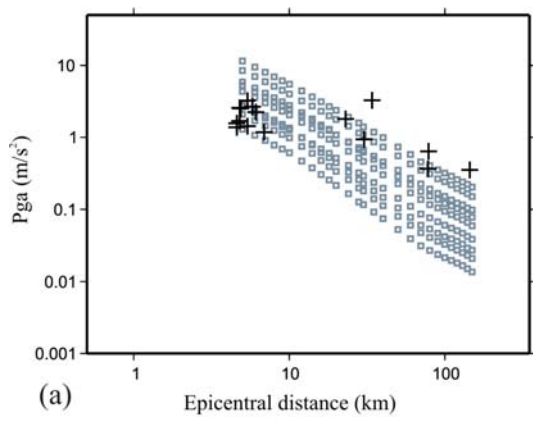


Fig.6

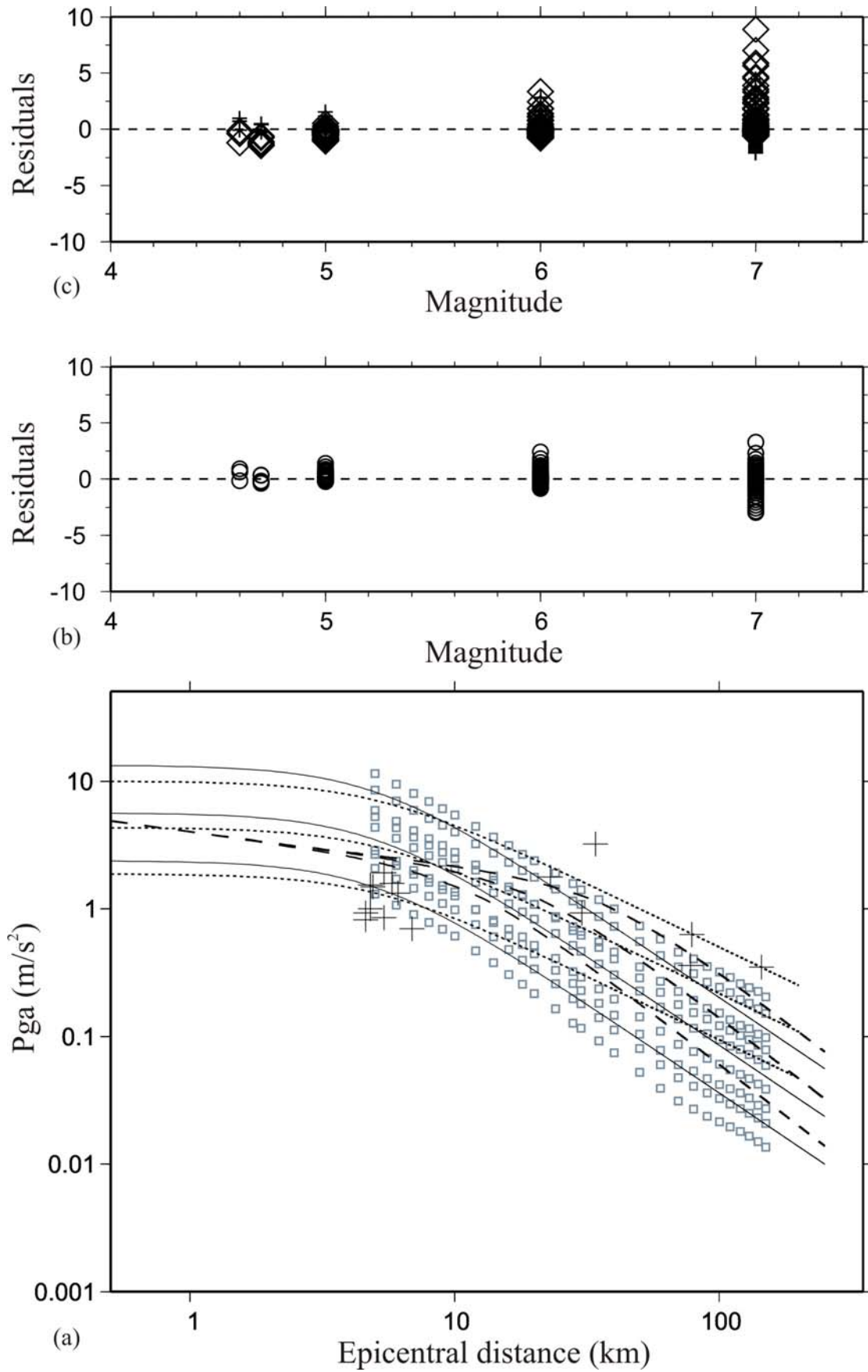


Fig. 7

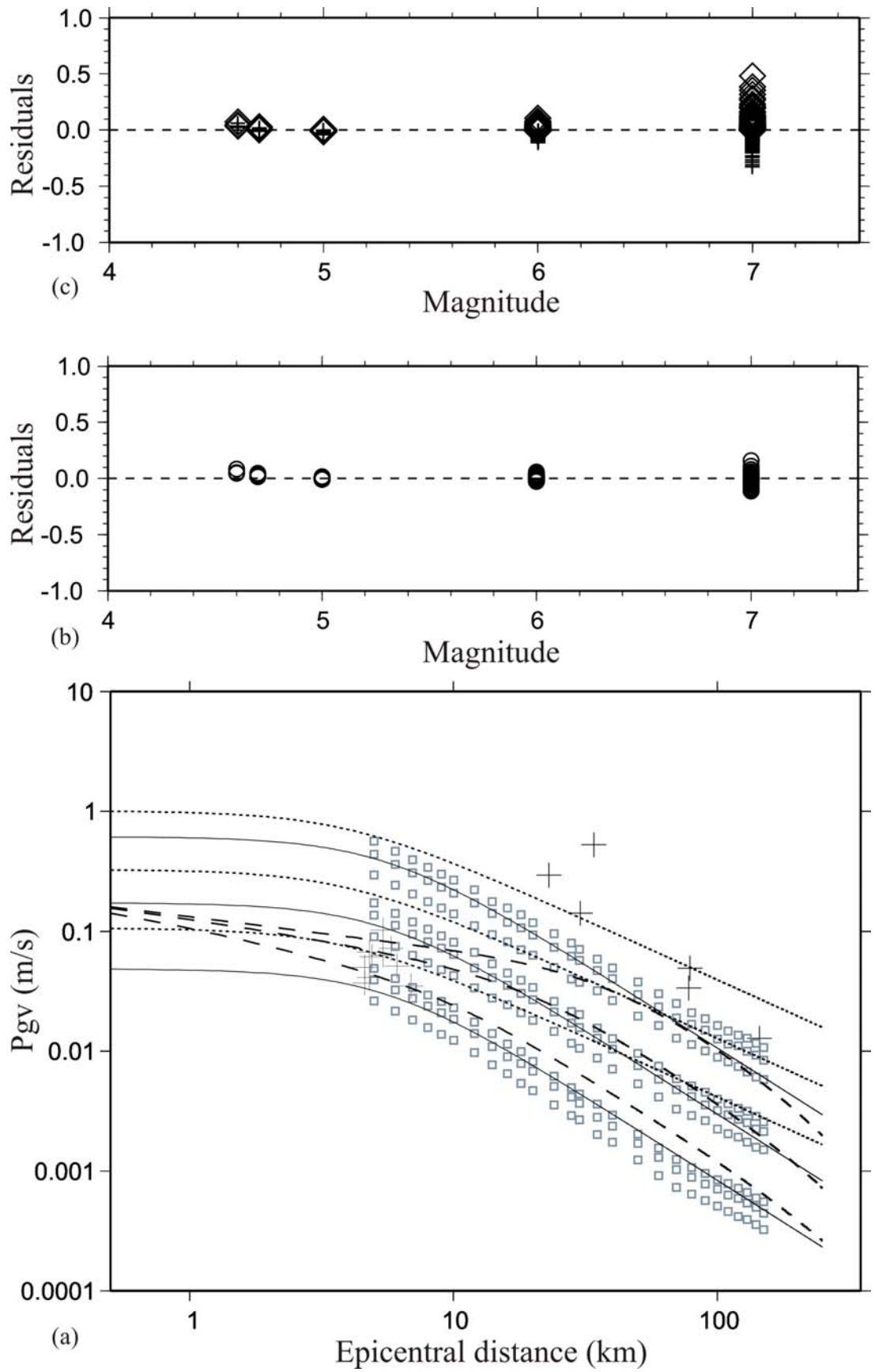


Fig.8

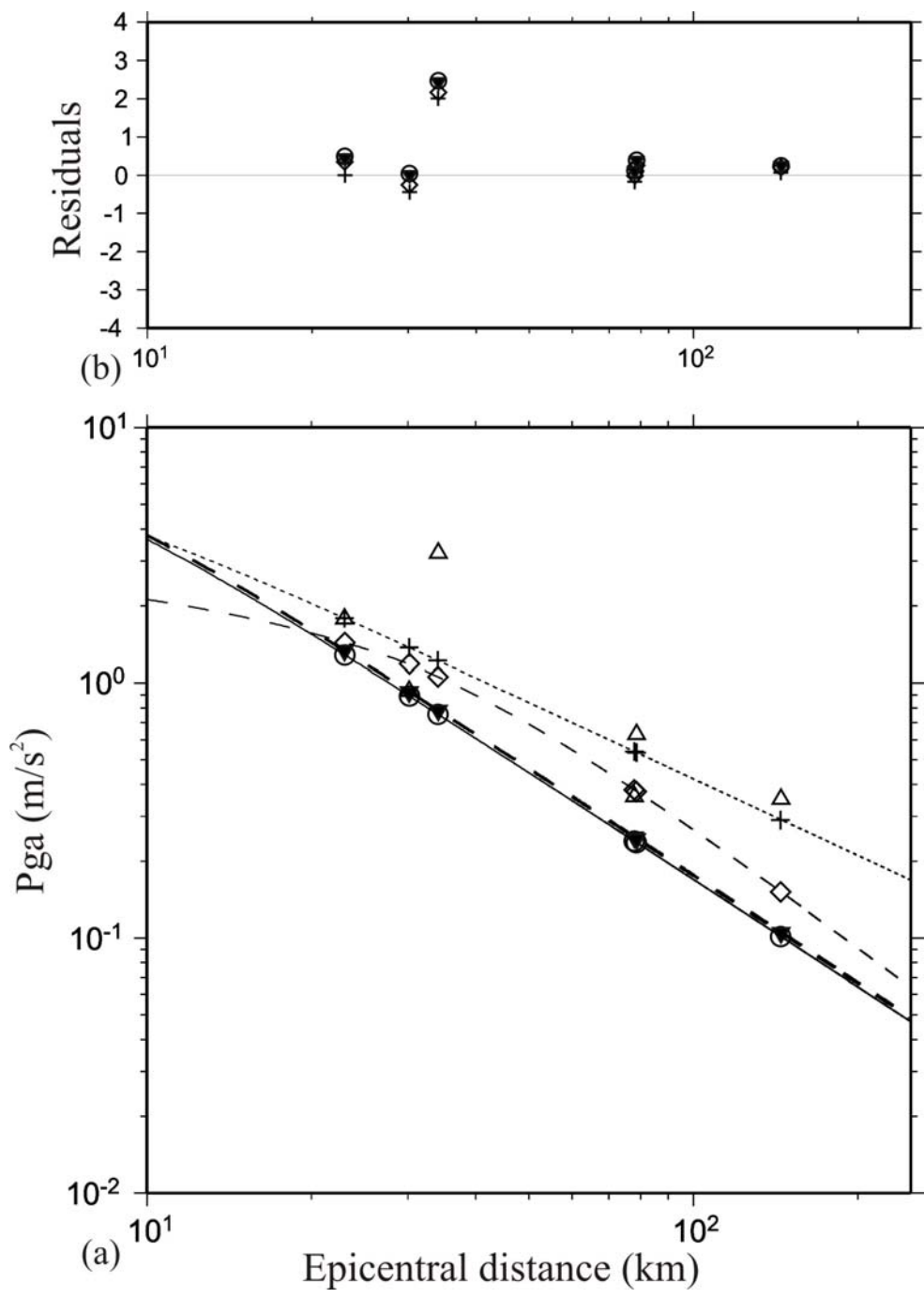


Fig.9

